Estuarine, Coastal and Shelf Science 126 (2013) 23–33

Contents lists available at SciVerse ScienceDirect

Estuarine, Coastal and Shelf Science

journal homepage: www.elsevier.com/locate/ecss

Particle size characterization of historic sediment deposition from a closed estuarine lagoon, Central California

Elizabeth Burke Watson [a,*], Gregory B. Pasternack [a], Andrew B. Gray [a], Miguel Goñi [b], Andrea M. Woolfolk [c]

[a] Department of Land, Air & Water Resources, 228 Veihmeyer Hall, University of California, Davis, CA 95616, USA
[b] College of Oceanic and Atmospheric Sciences, Oregon State University, 104 COAS Administration Building, Corvallis, OR 97331, USA
[c] Elkhorn Slough National Estuarine Research Reserve, 1700 Elkhorn Rd., Watsonville, CA 95076, USA

ARTICLE INFO

Article history:
Received 22 May 2012
Accepted 2 April 2013
Available online 18 April 2013

Keywords:
sediment sorting
sediment texture
granulometry
lagoon sedimentation
intermittently open estuaries
ICOLL

ABSTRACT

Recent studies of estuarine sediment deposits have focused on grain size spectra as a tool to better understand depositional processes, in particular those associated with tidal inlet and basin dynamics. The key to accurate interpretation of lithostratigraphic sequences is establishing clear connections between morphodynamic changes and the resulting shifts in sediment texture. Here, we report on coupled analysis of shallow sediment profiles from a closed estuarine lagoon in concert with recent changes in lagoon morphology reconstructed from historic sources, with a specific emphasis on the ability of suite statistics to provide meaningful insights into changes in sediment transport agency. We found that a major reorganization in lagoon morphology, dating to the 1940s, was associated with a shift in sediment deposition patterns. The restricted inlet was associated with deposition of sediments that were finer, less negatively skewed, and less leptokurtic in distribution than sediments deposited while the lagoon had a more open structure. These shifts are associated with a change in transport process from fluvial (through-flow) to closed basin (trapping). We also found other chemostratigraphic changes accompanying this shift in sediment texture, reflecting changes in organic matter source, wetland species composition, and an increase in sediment organic content, as presumably coarse, well-ventilated floodplain sediments tend to result in mineralization rather than sequestration of organic matter. In conclusion, we found that grain size analysis, in concert with the suite statistics technique, reflected changes in coastal configuration supported by historic maps and photos, however, we also recognize that this analysis was more informative given further context through additional sedimentary analyses. These findings provide a basis for the interpretation of particle size distribution in lithostratigraphic sequences associated with bar-built estuaries, where understanding natural and anthropogenically-modified inlet dynamics may help shape conservation management where concerns exist with respect to fish passage, water quality, and sediment transport.

Published by Elsevier Ltd.

1. Introduction

Grain size is the most basic physical property of sedimentary deposits (McManus, 1988; Poppe et al., 2000). The bed-surface sediment grain size spectra from individual depositional environments vary as a result of the particle size distribution (PSD) of parent material, selective and destructive transport processes, and the hydrodynamic characteristics of deposition (Friedman and Sanders, 1978). At the site of sediment origin, climatic and weathering processes, vegetation and slope interact with parent lithology to produce a mélange of detrital grains and secondary clay minerals (Weltje and von Eynatten, 2004), which are further modified by sorting, abrasion, or chemical alteration that occurs during transportation and episodes of temporary storage (Johnsson and Meade, 1990). At the site of accumulation, PSD is a response to the characteristic range of energy conditions necessary for transportation and deposition (Sahu, 1964). Thus, analyzing PSD may assist in reconstructing the site of origin, transport, and depositional processes associated with sedimentary deposits, from which further information about watershed processes and the geomorphic setting of the depositional environment can be derived.

* Corresponding author. Current address: ORD-NHEERL, U.S. Environmental Protection Agency, 27 Tarzwell Dr., Narragansett, RI 02882, USA.
E-mail addresses: elizabeth.b.watson@gmail.com, Watson.Elizabeth@epa.gov (E.B. Watson), gbpast@ucdavis.edu (G.B. Pasternack), abgray@ucdavis.edu (A.B. Gray), mgoni@coas.oregonstate.edu (M. Goñi), amwoolfolk@gmail.com (A.M. Woolfolk).

0272-7714/$ – see front matter Published by Elsevier Ltd.
http://dx.doi.org/10.1016/j.ecss.2013.04.006

Analyses of the PSD of sediment samples collected from coastal environments have been used to "finger-print" sub-environments (Glaister and Nelson, 1974), assess interactions between aeolian and tidal processes (Greenwood, 1969), and identify episodes of erosion and deposition in fore-shore environments (Hartmann and Christiansen, 1992). Specific approaches have included scatterplots of descriptive statistics and metrics such as graphic mean and inclusive graphic standard deviation (Folk and Ward, 1957; Folk, 1974), quartile deviations and medians (the QDa-Md method; Buller and McManus, 1972; Duck, 1994), mean-cubed deviation and simple sorting and skewness measures (Friedman, 1967), and descriptive statistics derived from log-hyperbolic and log-skewed Laplace distributions (Bagnold and Bardorff-Nielsen, 1980; Fieller et al., 1984, 1992). Briefly, these techniques characterize PSD by identifying central tendency and measuring spread as a difference from idealized distributions (e.g. log-normal). These metrics have also been used in concert with linear or non-parametric discrimination models (Sutherland and Lee, 1994), logistic regression (Vincent, 1986) and transport models (sediment trend analysis; e.g. Poizot et al., 2008) to discriminate between subenvironments of shorelines and reconstruct sediment transport patterns.

However, several critiques published during the 1980s and 1990s questioned the utility of using particle size analysis to ascribe specific sub-environments to sedimentary facies (Sedimentation Seminar, 1981; Erlich, 1983), and generally concluded that particle size data were inadequate as a sole means of paleoenvironmental reconstruction (Gale and Hoare, 1991). This led to a near-cessation of sedimentary studies presenting traditional textural analyses (Hartmann and Christiansen, 1992). Nevertheless, over the last decade as both laser granulometry and multiproxy paleoenvironmental reconstructions have become more common, studies are returning to the descriptive metrics of Folk (Lario et al., 2002; Priju and Narayana, 2007) and Friedman (de Carvalho et al., 2006) to provide meaningful insight into past environmental conditions.

The purpose of this study was to test the ability of the descriptive statistics and domains defined by Tanner (1991a; 1991b) to identify geomorphic and sedimentary processes using PSD data from shallow sediment cores collected from a coastal lagoon in Central California. During historic times, the geomorphologic structure of this lagoon has evolved from a floodplain wetland with some estuarine character (1850s–1910), to an open, relatively high-energy lagoon (1910–1930s), to a closed estuary largely filled with sediment (1940s-present). Our objective was to assess the interplay of lagoon morphology PSD to test the utility of grain size analysis in general, and Tanner domains in particular, for reconstructing changes in fluvial and depositional processes. More specifically, this study tests the ability of suite statistics to reconstruct prolonged episodes of inlet closure, a potentially important application for coastal settings where inlet management is common, yet knowledge about natural closure patterns is nearly nonexistent.

2. Study area and methods

2.1. Study area

The semi-arid Salinas Basin is the largest watershed on the central coast of California, draining a land area of 10,775 km^2 (Carter and Resh, 2005). Topography in the basin consists of steeply sloped uplands in the Santa Lucia and Gabilan ranges, with elevation peaks of ~1500 m, converging to a gently inclined fertile valley bordered by sloping terraces and alluvial fans (Fig. 1). The Salinas flows north-northwest for 250 km toward Monterey Bay. At the river mouth, the connection with the Pacific Ocean is closed most of the year by an impounding sand bar (Fig. 1; Farnsworth and Milliman, 2003) which is breached by the Monterey County Water Resources Agency when significant flow events develop (Watson et al., 2001).

Both current observations and historic accounts describe the mouth of the Salinas River as an intermittently closed lagoon open to the ocean during infrequent large events, and occasionally remaining open for several months (Johnson and Rodgers, 1854; Hermann, 1879; MacGinitie, 1935; Smith, 1953). The key difference between more natural configurations which existed prior to 1900

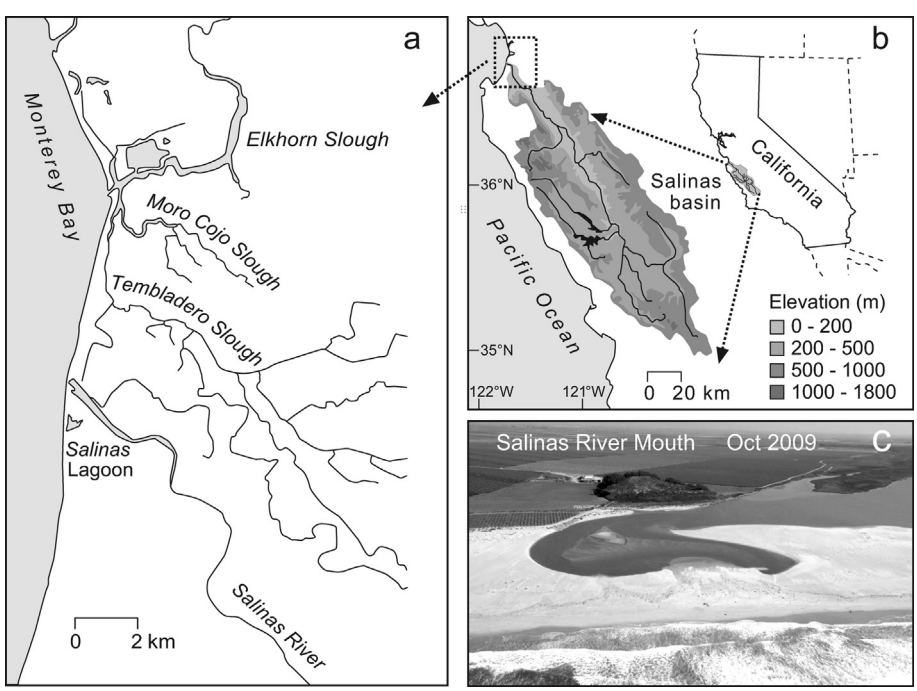

Fig. 1. Location map showing (a) the geography of the river mouth; (b) the Salinas Basin; and (c) the contemporary mouth of the Salinas River (source: Coastal Records Project, 2009).

and the situation today, is that the lagoon naturally drained to the north (Trask, 1854). Today, a network of water control structures largely restrict northerly through-flow. Channel avulsion events associated with episodic floods periodically reorganized the morphodynamics of the lagoon, which resulted in a more open or high-energy configuration during the early part of the last century (Fig. 2). During the early historic period and prior to 1910, the river veered northward as it neared the coast. Following a channel avulsion event in the early 1900s that straightened the approach to the coast, the lagoon became more fully open to the ocean through the 1920s and 30s. Infilling occurred in the 1940s, and since then the basic structure of the lagoon has been fairly constant, with alternating cycles of erosion and deposition.

2.2. Methods

2.2.1. Sample collection and processing

To document adjustments in sediment composition and texture resulting from changes in lagoon structure, shallow sediment cores were collected from six sites thought to have experienced deposition over the past century. A main core of 40-cm in length (SRL1) was collected in May of 2007 using a vibracorer. In Sept. of 2007, five additional box cores were collected (SRL 2–6). These box cores were 30–32 cm in length, and were collected at the vertices of a loosely arranged grid (Fig. 2). Although not all analyses were applied to all cores, the purpose of collecting multiple shallow cores was to determine the extent of spatial variability in sediment grain size (Wheatcroft and Butman, 1997), and to ensure that conclusions drawn from analyses of one core applied to a broad area rather being location-specific (Reavie and Baratono, 2006).

Several analyses were applied to the lagoon cores to establish deposition rates and aid in stratigraphic interpretation. First, sediment cores were split, described, photographed, and x-rayed. Each interval (representing one to two cm following natural breaks in lithology) was sampled for organic content (Heiri et al., 2001) and grain size determinations (Gray et al., 2010). To determine weight percent organic matter, one cubic cm subsamples were collected, dried, weighed, then combusted at 550 °C for 4 h, prior to re-weighing. Sediments sub-sampled for grain size analysis were treated over several hours with multiple aliquots of heated hydrogen peroxide to dissolve fine and coarse organic particles (Gray et al., 2010), dispersed with a 5% solution of sodium hexametaphosphate, disaggregated by briefly mixing on a vortex mixer, then agitated for 24 h at low frequency on a modified sieve shaker. Samples were then run through a Coulter LS230 laser granulometer with polarization differential intensity of scattered light (PIDS) for resolution to 0.045 μm. Relative volume of each sample was calculated with reference to standard USDA bin sizes

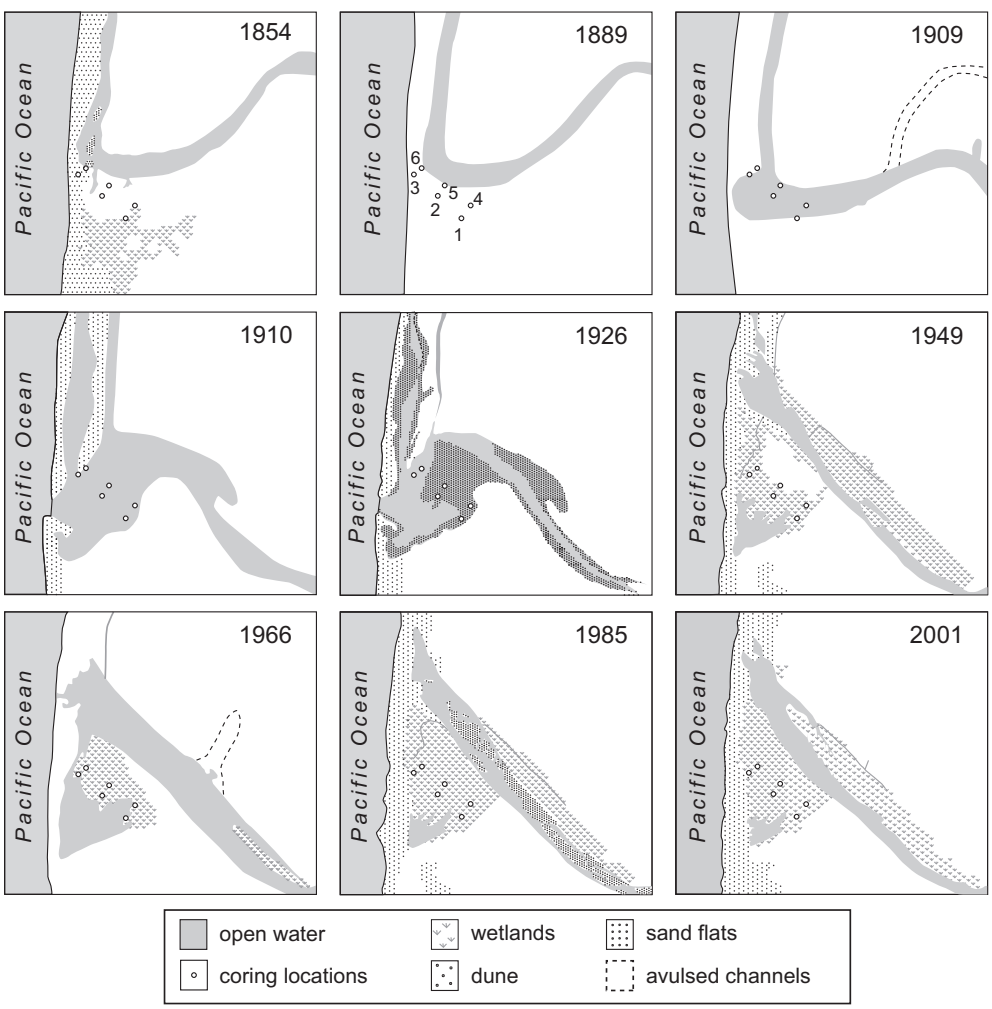

Fig. 2. Lagoon structure mapped from historic sources for the past two centuries, with coring locations indicated. (sources: U.S. Coast Survey, 1854; U.S. Coast and Geodetic Survey, 1889; Monterey County, 1909; U.S. Coast and Geodetic Survey, 1910; U.S. Coast and Geodetic Survey, 1926; U.S. Department of Agriculture, 1949; U.S. Department of Commerce, 1966; WAC Corporation, 1985; Monterey County, 2001). The 1889 lagoon map shows coring locations (SRL1, SRL2, SRL3, SRL4, SRL5, and SRL6).

Table 1
Salinas lagoon sediment core descriptions by stratigraphic zone.

Core zone	Depth (cm)	Density (g cm^{-3})	PSD mode (μm)	Texture	% Org.	Notes
SRL1-A	0–3	0.70	16	Mud	28.7	*Salicornia* roots/rhizomes
SRL1-B	3–4	1.05	17	Silty/v. fine sandy mud	8.8	
SRL1-C	4–7	1.05	130	Silty v. fine sand	7.9	Abundant biotite
SRL1-D	7–8.5	1.13	161	Silty medium sand	3.4	
SRL1-E	8.5–11	0.65	161	Muddy medium sand	16.9	
SRL1-F	11–12	0.73	2.5	Clay	13.5	
SRL1-G	12–14	0.97	122	v. fine sandy mud	9.2	
SRL1-H	14–15	1.44	147	Silty medium sand	5.0	
SRL1-I	15–17	1.29	101	v. fine sandy silt	4.7	
SRL1-J	17–42	1.35	179	Silty medium sand	1.2	
SRL2-A	0–13	0.89	4.0	Mud	16.6	*Salicornia* roots/rhizomes
SRL2-B	13–16	0.93	2.6	Clay	11.1	
SRL2-C	16–31	1.51	87	Silty v. fine sand	4.1	Abundant biotite
SRL3-A	0–2	0.72	3.2	Mud	30.8	*Salicornia* roots/rhizomes
SRL3-B	2–4	0.98	493	Medium sandy mud	13.1	
SRL3-C	4–9	1.08	411	Muddy medium sand	9.4	Abundant biotite
SRL3-D	9–17	1.43	497	Silty medium sand	3.4	
SRL3-E	17–27	1.47	735	Coarse sand	1.6	
SRL3-F	27–30	1.52	33	v. fine sandy silt	4.1	
SRL4-A	0–12	1.08	17	Mud	13.6	*Salicornia* roots/rhizomes
SRL4-B	12–16	1.37	53	v. fine sandy silt	6.5	
SRL4-C	16–19	1.26	84	Silty v. fine sand	4.1	
SRL4-D	19–25	1.50	76	v. fine sandy silt	4.3	
SRL4-E	25–31	1.35	78	Silty very fine sand	4.2	
SRL5-A	0–12	1.09	17	Mud	15.0	*Salicornia* roots/rhizomes
SRL5-B	12–15	1.19	76	v. fine sandy silt	6.9	
SRL5-C	15–18	1.32	122	Silty v. fine sand	3.0	Abundant biotite
SRL5-D	18–20	1.24	76	v. fine sandy silt	2.4	
SRL5-E	20–26	1.32	77	Silty v. fine sand	3.9	
SRL5-F	26–28	1.13	73	Fine sandy silt	3.9	
SRL5-G	28–30	1.29	37	Silty medium sand	3.2	Abundant biotite
SRL6-A	0–18	1.05	10	Mud	12.2	*Salicornia* roots/rhizomes
SRL6-B	18–20	1.27	25	Silt	6.5	
SRL6-C	20–23	1.49	409	Silty medium sand	1.5	Abundant biotite
SRL6-D	23–28	1.40	133	Silty fine sand	2.2	
SRL6-E	28–31	1.24	133	Silty v. fine sand	2.5	

(Coulter Co., 1994), and subsequently converted from the μm-scale to the ϕ-scale in order to make comparisons with established methods (Folk, 1974). Nomenclature of grain size distributions follows Folk (1974).

To provide chronologic control, one of six surface cores (SRL1) was dated using radiometric dating techniques and analyzed for historical geochemical markers. Sediments were analyzed for Pb-210, Cs-137, and Pb-214 (used to determine unsupported Pb-210 activity) using a Canberra GL2020RS low energy geranium planar gamma ray detector. For each interval, sediments were also analyzed for bulk geochemistry using ICP-AES, with pretreatment by four-acid near-total digestion. The sediment lead concentration peak was assigned a date of 1974, coincident with the beginning of the phase-out of leaded gasoline and sediment lead peaks found in other Californian sediment cores (Finney and Huh, 1989). This chronology was then refined based on the presence of historic flood deposits (Pasternack et al., 2009). Flood deposits were recognized from visual and x-radiograph examination of prominent laminations, shifts in sediment PSD and geochemistry, and from pollen analysis, and were assigned to historic events based on analysis of peak flow events recorded at the most downstream gauge on the Salinas River (USGS 11152500, Salinas River near Spreckles, USGS, 2010).

For two of six surface cores (SRL1 and SRL6), sediments were sub-sampled and analyzed for pollen spectra and abundance (Faegri and Iversen, 1975). In order to facilitate calculations of total absolute pollen concentration, tablets containing a known number of *Lycopodium* spores were introduced (Stockmarr, 1971). Pollen identification was made on a Nikon Eclipse E200 microscope, at 400 times magnification and with reference to published pollen atlases (McAndrews et al., 1973; Kapp et al., 2000). Variations in pollen concentration have been used to successfully resolve variability in the rates of sediment accumulation (Defries, 1986; Brush, 1989; Cooper and Brush, 1991; Pasternack et al., 2001; Constantine et al., 2005). Briefly, assuming that pollen deposition is derived from mainly atmospheric sources, then intervals of rapid sediment accumulation correspond to low pollen sediment pollen concentrations; conversely, intervals of low sediment accumulation correspond with high pollen sediment concentrations. This relationship has been formalized using the following equation:

$$R_i = \left(\frac{\overline{n}}{n_i}\right)\overline{R}\rho_i$$

where R_i is the sedimentation rate of interval i in g cm^{-2} yr^{-1}, $\overline{n}$ is the average number of pollen grains per unit volume between dated horizons, n_i is the total number of pollen grains per unit volume in interval i, $\overline{R}$ is the average sediment rate based on dates derived from other methods, and ρ_i is the sample bulk density. Using this equation, high resolution accumulation rates between intervals of known dates were calculated between 1954 and 2007.

Core SRL1 was also analyzed for carbon and nitrogen content (both with and without pre-treatments to remove inorganic carbon) using a Thermo Quest EA2500 Elemental Analyzer. Sedimentary organic matter in this core was further analyzed for stable isotopes of carbon and nitrogen. Stable isotope ratios are expressed in per mil notation, such that, for each sample $\delta^{13}C = (R_{sample} - R_{standard})/$

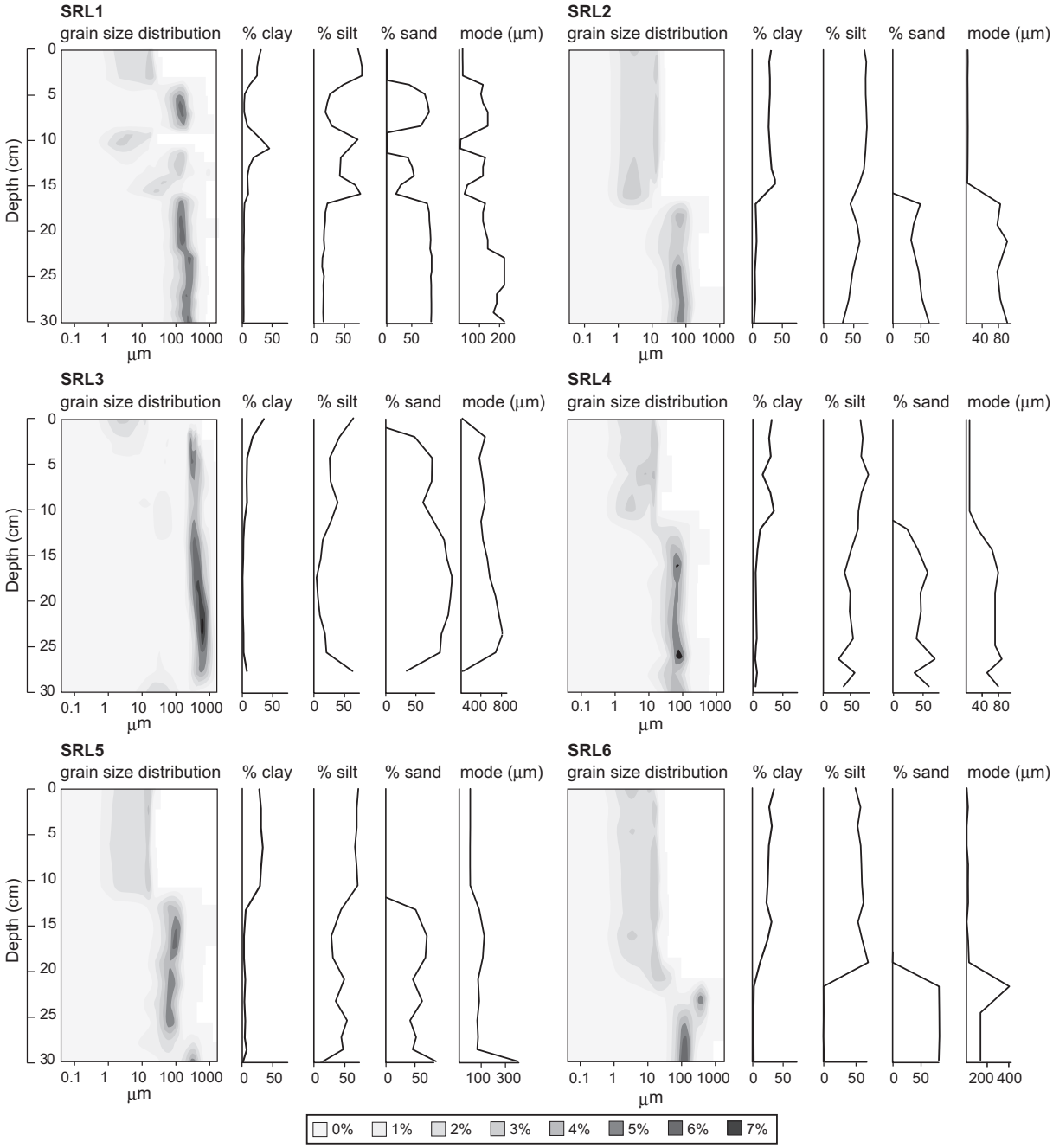

Fig. 3. Particle size distribution for Salinas River Lagoon cores.

$R_{standard} \times 1000$, where R is the molar ratio of the less common to the more common isotope.

For comparison, suspended load samples were also collected from the lower Salinas River during flow events from 2008 through 2010. Suspended sediment samples were collected during events, rather than by regular intervals, due to the highly episodic nature of discharge on the Salinas River. Our intention was to collect multiple samples from every discharge event (e.g. rising, peak, and falling hydrograph limbs). Water samples of 2 L in volume were retrieved from the water surface at across channel stations of approximately one quarter, one half, and three-quarters across the active channel width. Water samples were analyzed for total suspended sediment concentration by filtering a known volume of water through a pre-combusted glass fiber filter, and particle size distribution analysis using methods described above.

2.2.2. Data analysis

To describe sediment size and level of processing (or sorting), graphic expressions were calculated for each sample, including graphic mean, inclusive graphic standard deviation, inclusive graphic skewness, and kurtosis (Folk, 1974). These expressions, and associated suite statistics, such as the standard deviation of mean particle size in a sediment pool, have been used by Tanner (1991a; 1991b), as well as other investigators (Lario et al., 2002), to identify characteristics of the sediment transport agency. This includes associating various characteristics of grain size distributions with transport regime comparisons, such as air vs. water, back-and-forth

Table 2
Sample grain size (ϕ), showing graphic mean, inclusive graphic standard deviation, skewness, and kurtosis for basal and surface sediments.

	Surface sediments average (range)	Basal sediments average (range)
Mean (ϕ)	7.36 (3.17–8.91)	3.52 (0.66–7.34)
Standard deviation	1.79 (1.33–2.78)	1.68 (0.96–3.42)
Skewness	−0.17 (−0.058–0.09)	−0.38 (−0.82–0.25)
Kurtosis	0.95 (0.6–1.68)	1.39 (0.58–2.81)

shuffling vs. unidirectional sediment transport, and flow-through vs. trapping. The suite statistics method uses the position of samples within bivariate plots (such as sample skewness vs. mean) to compare the sediment pool with the transport agency domains discriminated by Tanner using empirical calibration. Here, we plot samples in bivariate spaces defined by distribution characteristics to compare suite statistics classifications to historic changes in lagoon morphology. Additionally, we formally test for significant differences among mean values of sample distribution properties before and after the 1940s shift in lagoon structure. In addition, changes in the relationship between grain size and sorting coincident with lagoon closure were formally compared by testing for differences in the slope of the fitted curve calculated using linear regression methods; site-to-site differences were compared using analysis of covariance.

3. Results

3.1. Core lithostratigraphy

Variations in lithologic and organic characteristics were observed throughout the length of the cores. For the purposes of discussion, the sediment profiles were divided into zones characterized primarily by lithostratigraphy (Table 1). Nomenclature of grain size classifications follows Folk (1974).

3.2. Particle size distribution

Analysis of surface cores for sediment grain size demonstrated a pronounced shift in sediment deposition patterns (Fig. 3; Table 2). Deeper sediments were composed of a mixture of fine and medium grains (e.g. silty fine sand), while surface sediments were found to be composed primarily of fines (a mixture of silts and clays, termed

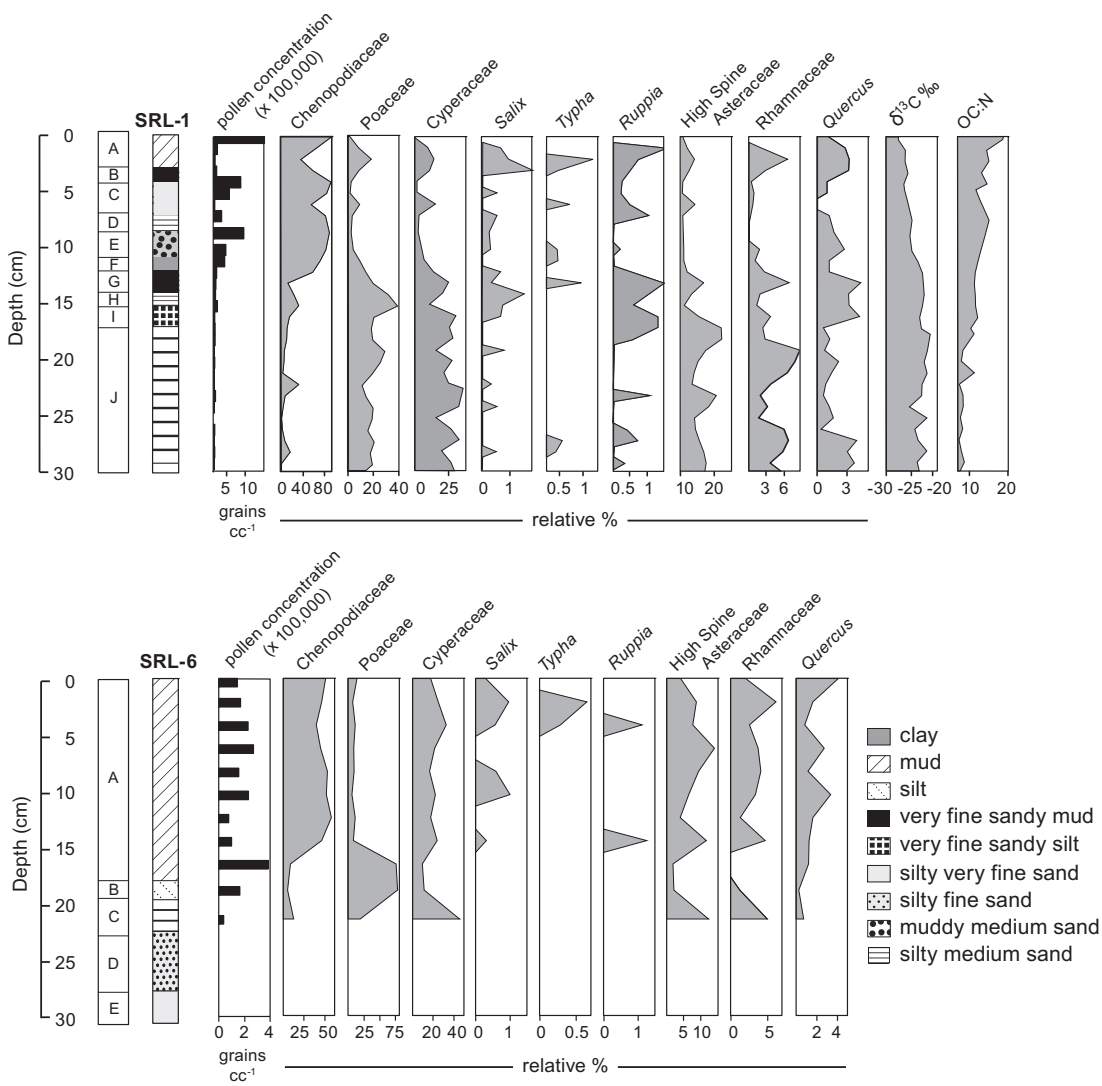

Fig. 4. Results of pollen analysis for Salinas River sediment cores.

mud). The downcore shift in sediment deposition was found at 12–17 cm of depth (apart from that of core SRL3) and was accompanied by an increase in organic content, a decrease in density, changes in the character of organic matter, and a change in pollen spectra (Fig. 4). In addition, fluvial suspended sediment and bed-surface lagoon sediments displayed similar particle size distributions (Fig. 5). Bimodal peaks in the 3.7 and 15 μm size classes dominated the particle size distribution for suspended and lagoon surface sediments, and were labeled as fine (very fine silt), poorly sorted, coarse-skewed, with platykurtic distributions (i.e. flat-peaked distributions in which the population extremes are better sorted than the means). For the lagoon samples, the coarse peak was more prominent, suggesting that higher energy flow events are responsible for depositing sediments in the lagoon wetlands.

Deeper and coarser lagoon samples were more diverse. With very few exceptions, coarse samples had a uni-modal distribution pattern. The grain size mode for each sample varied between 25 and 500 μm, and the grain size distribution typically included a long fine tail. The most common grain size mode (for about $^1/_3$ of samples) was the 100–200 μm size class. Thus, coarse sediments were poorly to very poorly sorted, strongly positively skewed due to long fine tails, and leptokurtic (a peaked distribution where the center of the distribution is better sorted than the extremes). Cores SRL1, SRL2, SRL3, and SRL 4 also had a fining-upwards sequence. Core-to-core comparisons found that deeper sediments were finer relative to other coring sites for cores SRL2, SRL4, and SRL5, with the coarsest sediments found at the base of core SRL3. The contrasts in grain size distributions among cores are related to the geographical location of each site. Cores SRL3 and SRL6 were collected close to the beach front and historic inlet, whereas core SRL1 was collected from the historic lagoon margin. These sites were likely to have experienced historically more energetic conditions capable of transporting larger particle sizes.

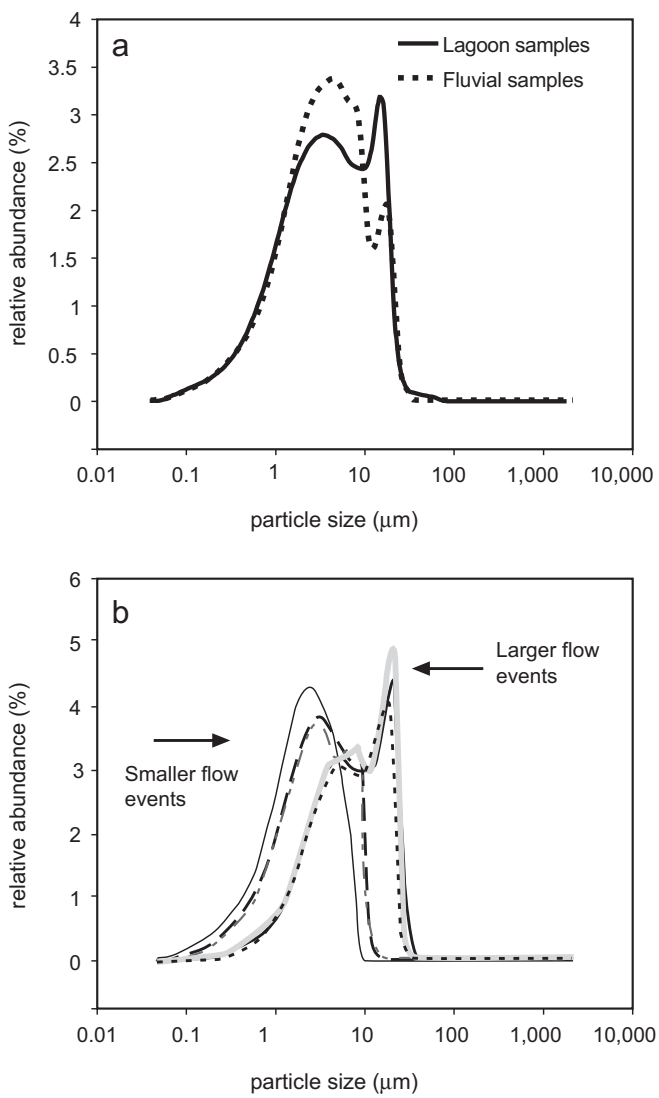

Fig. 5. 5a. Average grain size distribution of sediment samples collected from the lagoon ($n = 34$) and from the river channel ($n = 15$). Fluvial samples derive from suspended sediment samples; lagoon sediments from bed-surface samples. 5b. Fluvial samples from different size flow events. Within the context of small events, with a yearly return frequency, grain size generally scales with flow, however for subsequent analyses conducted for heavier rainfall years with flow events that differ in magnitude, grain size often responds more strongly to other factors: there appears to be a legacy effect from previous events, and storm hydrology also appears to be important (i.e. which part of the basin is contributing flow).

More variability was found in sample-specific sorting and kurtosis values for basal sediments than for surface sediments. Moreover, the relationship between sample-specific grain size and sorting also appears to have undergone a pronounced shift (Fig. 6). A negative correlation was apparent between basal sediment grain size and sorting, while a positive correlation was found for surface sediments.

Core SRL1 was unique among the six cores described in that surface and near-surface fine sediments were prominently laminated; by closely comparing core photographs and x-rays with flow records, laminations were attributed to individual flood events (Pasternack et al., 2009). Field verification through additional surface coring confirmed that these laminations were consistently preserved in a wide area (up to tens of meters distant), although they were not found at other sites cored by this project. Examination of a flood map and air photos from the 1995 flood show that this site is situated on an abandoned channel, and thus appears to be impacted by flood deposition most consistently.

3.3. Chronology, flood layers, and supplemental analyses

For core SRL1, the peak in lead concentration (of 39 ppm) occurred at 11-cm of depth, while the first detectable radiocesium was found at a depth of 16 cm (Fig. 7). The Pb-210 record did not show a linear decline in unsupported activity, and therefore was not useful as a tool in chronology development. Flood layers were recognized in SRL1 based on laminations apparent visually and in x-radiographs, were apparent as relative minima in pollen concentration, and as maxima in sediment deposition reconstructed using pollen concentration methods. Flood deposits tended to be relatively homogenous in particle size distribution within a layer, but varied in grain size between deposits. Plotting flood layers in 2-D spaces defined by PSD characteristics indicated that flood layers are fluvial rather than beach deposits, such as may occur with dune overwash during storms (Fig. 8a;b;d). Separation of flood layers from adjacent deposits by poorly sorted transitional sediment layers was typical. Based on hydrologic records maintained by the U.S. Geological Survey in concert with the known isochronological markers reported above (1974 and 1954), we assigned flood layers found at 4, 7.5, 9.5, and 12 cm of depth to years 1995, 1983, 1978, and 1969, respectively. A linear regression equation generated using known age-depth pairs was found to have a slope of 0.329 cm y^{-1} and an r^2 value of 0.99. Using this accretion value to interpolate ages from deeper depths, it appears that the primary shift in grain size recorded by cores SRL 1–6 dates to between 1940 and 1950.

In SRL1 we also found a pronounced shift in the composition of sedimentary organic matter coincident with the change in lagoon morphology. The chemostratigraphic data indicated that lagoon

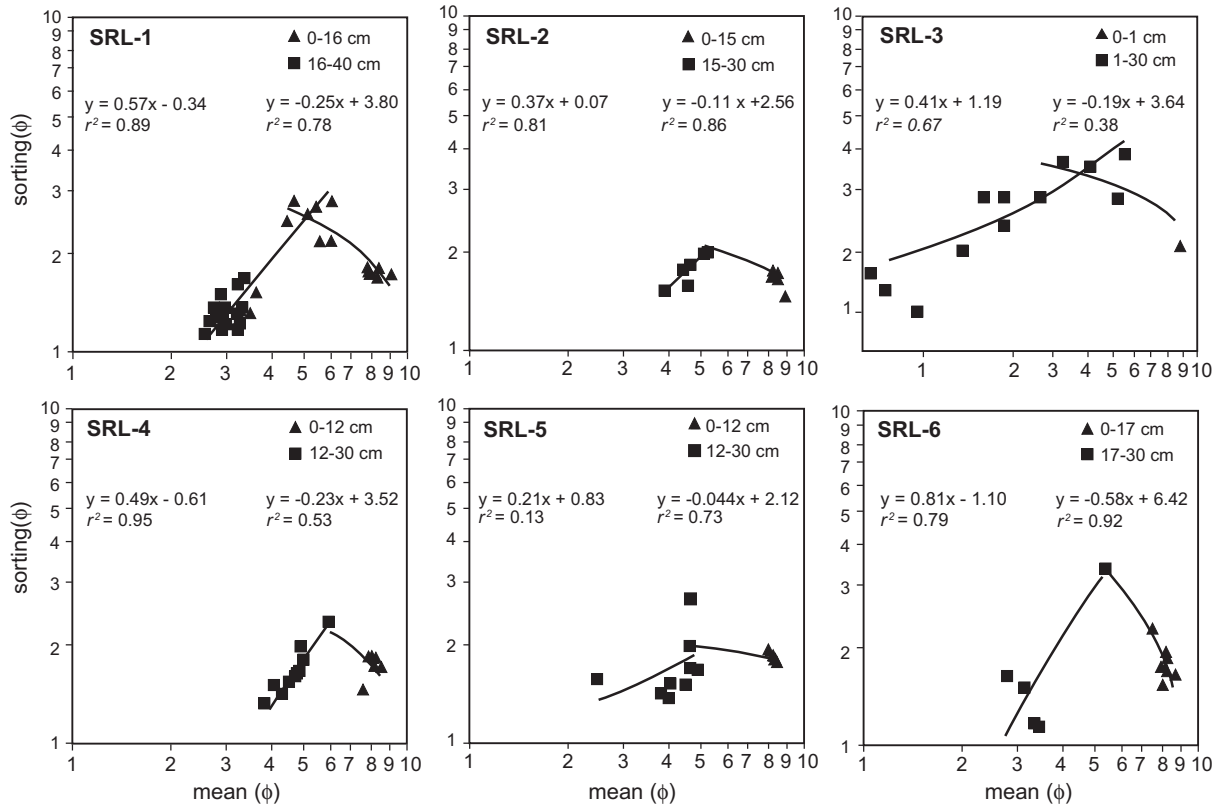

Fig. 6. Bivariate plots of mean grain size against sorting for all Salinas River Lagoon cores.

infilling was accompanied by an increase in the molar organic carbon to nitrogen ratio (OC/N) from 8.4 ± 1.4 in deeper sediments to 13.3 ± 2.0 in surface sediments (mean ± sd), and a decrease in $\delta^{13}C$ values from −22 ± 1.0‰ in deeper sediments to −25 ± 1.7‰ in surface sediments. The trend toward higher C/N vales and more depleted stable carbon isotope ratios in sediments shallower than 15 cm are consistent with an increase in the contributions from vascular land-plant sources, whereas the lower C/N values and enriched $\delta^{13}C$ values in deeper sediments are consistent with higher contributions from algal sources (Cloern et al., 2002; Goñi et al., 2008). This change in sedimentary organic matter source — from algal to terrestrial — coincides temporally with the closing of the direct connection with the ocean post-1940s (Fig. 2). Historical maps confirm this shift from open lagoon to a *Salicornia* marsh at the coring site during this period and support this chemostratigraphic interpretation. Notably, this change is unlikely to be a result of post-depositional alteration of the sedimentary organic matter because prolonged diagenesis often results in the preferential degradation of nitrogen-rich and isotopically-heavy biochemicals such as proteins relative to carbon-rich isotopically depleted biochemicals such as lignins (e.g. Ember et al., 1987; Gonneea et al., 2004; Zhou et al., 2006). Hence, we would expect the older sediments near the bottom of the core to have more carbon and $\delta^{13}C$ depleted compositions, opposite to what is observed.

Dominance of wetland pollen was found to have shifted from grass and sedge pollen (Poaceae and Cyperaceae pollen types, respectively) to primarily Chenopodiaceae pollen coincident with the shift in grain size for cores SRL1 and SRL6. For SRL1, this shift occurred from 20-cm of depth to 14-cm of depth, which can be dated to the 1940s through 1960s. This shift in pollen abundance is likely attributable to the establishment of the large *Salicornia* marsh (*Salicornia* is a member of the Chenopodiaceae plant family) during the 1930s through 1950s. Although historic maps do not allow definitive identification of plant species based on the wetland-type hatching, a report dating to the time period in question describes the vegetation and salinity regime of the Salinas Lagoon marsh (Smith, 1953), and identifies *Salicornia* as the dominant vegetation type.

4. Discussion

Recent studies of estuarine sediment deposits have focused on grain size spectra as a tool to better understand episodic or regime shifts in depositional processes on geologic timescales, in particular those associated with tidal inlet and basin dynamics (Baker et al., 2010; Wang et al., 2010). The key to accurate interpretation of lithostratigraphic sequences is establishing clear connections between morphodynamic changes (such as inlet progradation) and the resulting shifts in sediment texture, including measures of central tendency, and spread, such as those described by Folk (graphic mean, inclusive standard deviation, skewness, and kurtosis; 1974). Using paired analysis of historic sediment profiles and historic maps, this study sought to empirically establish a relationship between estuarine closure and sediment composition.

In order to compare changes in transport agency reconstructed from the approaches of Friedman (1967) and Tanner (1991a, b) with our knowledge of historic changes in lagoon structure, bivariate plots were constructed to compare surface (presumably post-1940s) against deeper sediments for all grain size samples, including mean vs. sorting, skewness vs. kurtosis, sorting vs. skewness, and suit standard deviation of mean vs. suite standard deviation of sorting. Using defined domains (Tanner, 1991a, 1991b; Lario et al., 2002), the shift in the relationship between sediment grain size and sorting indicates a shift in transport agency, from flood dominated to closed basin/estuarine deposition (Fig. 8a). Kurtosis plotted as a function of skewness suggests fluvial

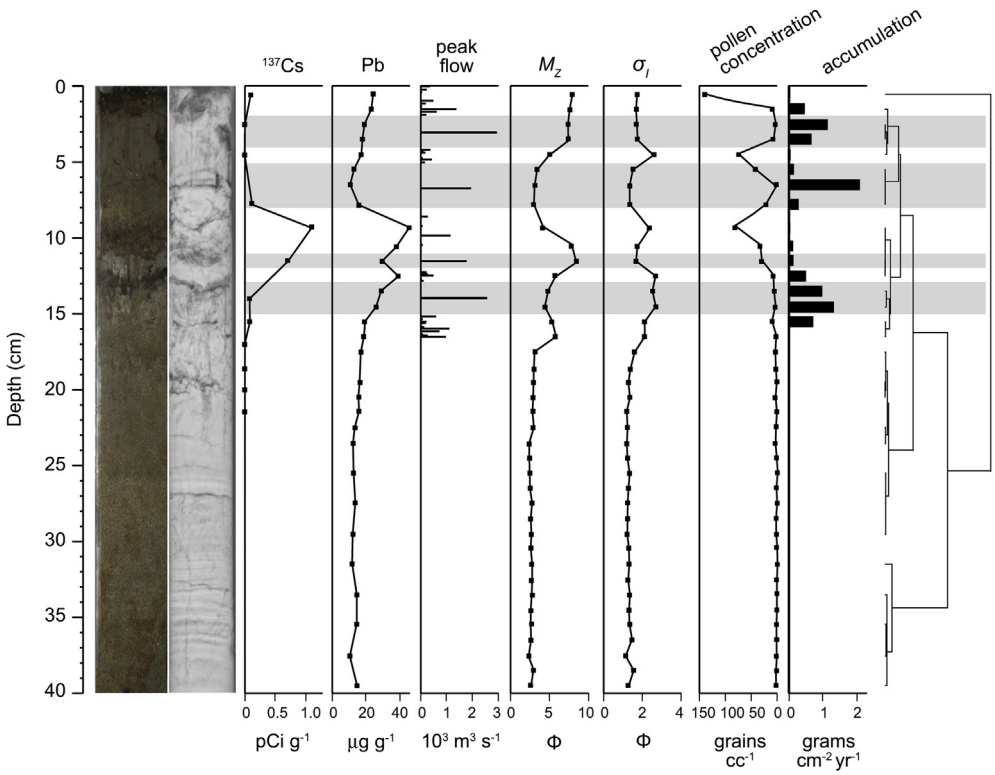

Fig. 7. Diagrams showing sediment core imagery and x-radiography, chronological markers including ^{137}Cs decay activity, total Pb concentration, yearly peak flow data from the most downstream Salinas River gauge, pollen concentration, pollen based sediment accumulation rates, particle size graphic mean (M_Z) and inclusive graphic standard deviation (σ_I) as a function of depth for core SRL1, which contained age-constrained historic flood deposits. Shaded depths are interpreted as flood deposits. Dendrogram shown at right was derived from a constrained cluster analysis performed on bulk geochemical data (LOI-free).

deposition (Fig. 8b) and an increase in sample skewness from basal to surface depths. A plot of inclusive graphic sample skewness standard deviation against the standard deviation of the inclusive graphic standard deviation (a "variability diagram") shows all values plotting on the fluvial portion of the diagram, and suggests a decline in stream energy through time. A plot of inclusive graphic skewness against sorting shows all samples plotting in the fluvial domain of Friedman (1967). A few samples (generally from core SRL3, the coring site closest to the beach fore-dune) are near the river/beach domain boundary (Fig. 8c, d).

With respect to sediment texture, bed surface sediment composition closely matched suspended sediment samples collected 15-km upstream over five separate flow events (Fig. 4). This implies that the source of sediments to the Salinas River lagoon is currently the wash load of the Salinas River. However, because the river sample average has a more prominent fine peak, we presume that the magnitude of the events responsible for much of the lagoonal sediment deposition are the larger of the smaller flow events (30 m^3s^{-1}, return interval of 1y; Casagrande and Watson, 2003). Examination of USGS stream gauge data, Monterey Bay wave buoy data, and water level data from the Salinas Lagoon (CDEC, 2010) indicated that larger events typically consist of two stages, with a lagoon filling stage originating from wave overtopping, followed by a (natural or artificial) breaching, lower water levels and tidal exchange through an oceanic inlet. Thus, larger flows, with proportionately coarser loads, are subject to sediment bypass during low tide, and upstream settling during high tides, while smaller events and the early low flows of larger events result in estuarine flooding. This interpretation explains the bulk of surface deposition for coring sites SRL2, SRL4, SRL5, and SRL6, where supra-tidal elevations generally do not permit submergence during lagoon open-conditions. However, the pattern of contemporary sediment texture for coring sites SRL1 and SRL3 indicates that lower marsh elevations continue to receive coarser sediment, at least episodically. Transport of coarse sediment to these coring sites implies a flow pathway during larger events that follows an historic channel meander (Fig. 2; 1966).

Deeper sediments are a mixture of fine and coarse sediments. Strong uni-modal peaks in the 60–200 µm range indicate moderately energetic conditions and some processing of sediment, probably through wave action during lagoon-open conditions. All sediment samples also possessed long fine tails, indicating settling conditions (and the absence of winnowing conditions; Tanner, 1991b), produced by lagoon-closed conditions. Contrasting surface with deeper sediments shows that the texture of deposited sediment fined rapidly over time. Comparing sediment composition with respect to pollen abundance indicates that this event took place coincident with the establishment of the *Salicornia* marsh, while radiometric data establishes that this fining in sediment composition occurred prior to the early 1950s. Thus the shift in grain size corresponds to lagoon infilling and *Salicornia* marsh establishment that occurred sometime between the 1920s and late 1940s.

This shift in sediment texture was accompanied by a change in the relationship between sediment size and level of processing: for samples with means coarser than 5ϕ, coarser samples were better sorted, while for samples with means finer than 5ϕ, finer samples were better sorted. Past studies have interpreted this shift in the particle size/sorting relationship as a change in transport agency from flood-dominated to closed basin (Lario et al., 2002; Switzer et al., 2005), however it has also been interpreted as resulting from the abundance of sand and clay particles in nature relative to silt (Folk, 1974): samples which have means or medians in the 5–6 ϕ size class would naturally be poorly sorted as they would consist

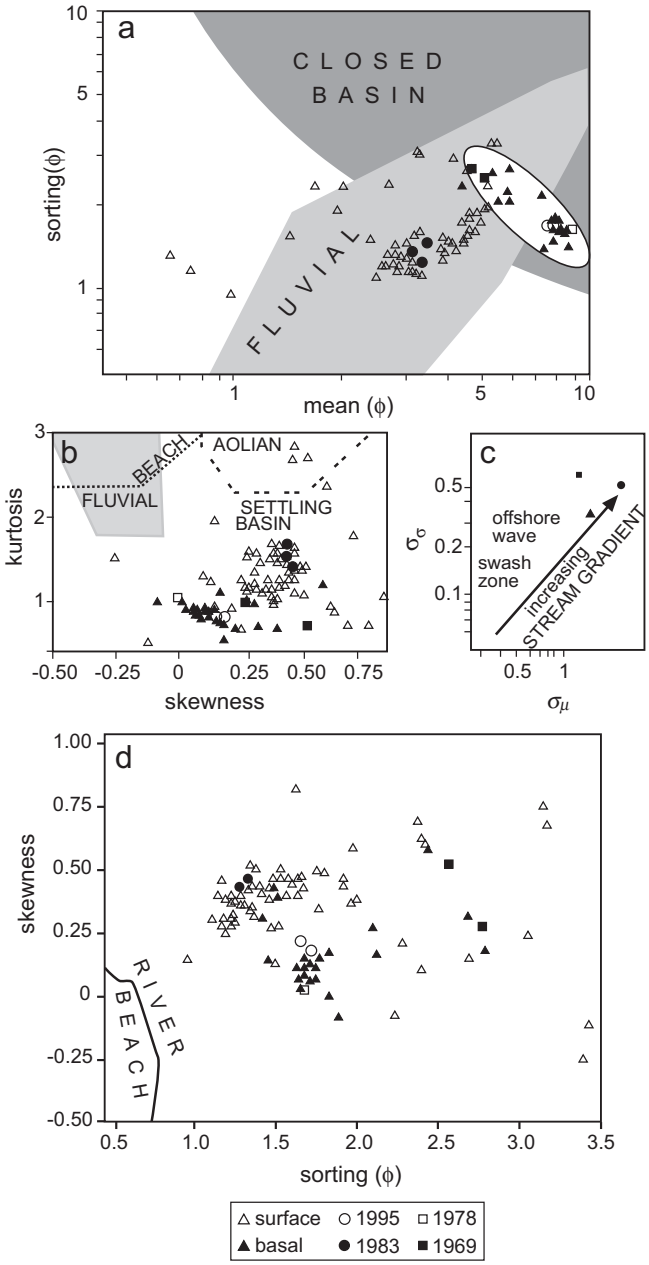

Fig. 8. Bivariate plots of grain size parameters plotted against the domains of Tanner (1991a; 1991b), Lario et al. (2002), and Friedman (1967): 8a. Graphic mean against inclusive graphic standard deviation (circle denotes partially open to restricted estuary; Lario et al., 2002), 8b. inclusive graphic skewness against kurtosis (beach domain is enclosed by a dashed line; fluvial domain by a shaded box), 8c. suite statistics: standard deviation of graphic mean against standard deviation of inclusive graphic standard deviation. Triangles indicate surface sediments, squares basal sediments, and the circle both, 8d. inclusive graphic standard deviation against inclusive graphic skewness.

of mixes of finer and coarser particles. Examination of an additional 400 samples collected from nearby lacustrine and estuarine environments shows nearly all samples following this pattern, with very few (<5%) outliers (Watson, unpublished data).

5. Conclusions

By mapping lagoon morphology during the late nineteenth and twentieth centuries using historic maps and aerial imagery, we reconstructed substantial changes in the morphology of the Salinas River Estuary, which has the largest watershed of any Central California coast river. While the Salinas Lagoon is generally only open to the ocean during and immediately after large storms, we found that the Lagoon briefly maintained a more open structure during the early twentieth century, and transitioned to more closed conditions after the 1940s. By analyzing shallow sediment profiles collected from the Lagoon for particle size distribution, we found that this shift from open-inlet conditions to more closed conditions was associated with a fining of sediment deposited in the lagoon, as well as shifts in other aspects of particle size distributions measured by skewness and kurtosis, as well as by the relationship between mean and sorting. These measures may have great value for studies of estuarine closure at other dynamic coastal sites of interest for stewardship, management, or restoration purposes, where closure history is less well-documented, inlet stability is recognized as an important consideration for salmonid conservation, sediment transport, water quality, or coastal flooding, and inlets are being actively managed, or active management plans are under consideration.

Inlet closure was also strongly associated with a shift in the source of sedimentary carbon. As the lagoon filled with sediment and wetlands were established, the carbon source switched from algae to terrestrial organic matter. Furthermore, the pollen record reflected the establishment of wetlands. In conclusion, textural distributions were found to reflect changes in coastal and fluvial conditions supported by historic research, but were found to be most useful given additional context, through additional sedimentary analysis and textural analysis performed on fluvial samples collected from the lower reaches of the river channel.

Acknowledgments

This research was supported in part by the National Science Foundation under award No. 0628385. Any opinions, findings, and conclusions or recommendations expressed in this material are those of the authors and do not necessarily reflect the views of the National Science Foundation. Thanks to Rob Wheatcroft for gamma spectroscopy, to Eric Van Dyke for assistance with historical ecology research, to Scott Morford, Katie Farnsworth, Sonja Gray, Francis Madden, Yvan Alleau, Larissa Salaki, Peter Barnes, Sarah Greve, and Duyen Ho for help with core collection and sample processing, to Ivano Aiello and Dave Schwartz for helpful discussions, and to Patricia DeCastro for assistance with graphics.

References

Bagnold, R.A., Bardorff-Nielsen, O., 1980. The pattern of natural size distributions. Sedimentology 27, 199–207.
Baker, D., Peterson, C., Hemphill-Haley, E., Twichell, D., 2010. Latest Pleistocene and Holocene (2-16 ka) sedimentation in the Columbia River estuary, Oregon, USA. Marine Geology 273, 83–95.
Brush, G.S., 1989. Rates and patterns of estuarine sediment accumulation. Limnology and Oceanography 34, 1235–1246.
Buller, A.T., McManus, J., 1972. Simple metric sedimentary statistics used to recognize different environments. Sedimentology 18, 1–21.
California Data Exchange Center, 2010. Hydrographic Data for Salinas River at Lagoon. September 2003-present. California Department of Water Resources, Sacramento, CA. online dataset. http://cdec.ca.gov.
Carter, J., Resh, V., 2005. Pacific Coast rivers of the coterminous United States. In: Benke, A.C., Cushing, C.E. (Eds.), Rivers of North America. Elsevier, Burlington, MA, pp. 541–590.
Casagrande, J., Watson, F., 2003. Hydrology and Water Quality of the Carmel and Salinas Lagoons Monterey Bay, California 2002/2003. Report to Monterey County Water Resources Agency, California, Report No. WI-2003-14. The Watershed Institute, California State University Monterey Bay, Seaside, CA, p. 128. http://ccows.csumb.edu/pubs/reports/CCoWS_LagoonBreaching2002-2003_030630.pdf.
Cloern, J.E., Canuel, E.A., Harris, D., 2002. Stable carbon and nitrogen isotope composition of aquatic and terrestrial plants. Limnology and Oceanography 47, 713–729.
Coastal Records Project, 2009. Oblique Aerial Photograph. N36'45.05°, W121'48.44° Image 200908310. http://www.californiacoastline.org/.

Constantine, J.A., Pasternack, G.B., Johnson, M.L., 2005. Logging effects on sediment flux observed in a pollen-based record of overbank deposition in a northern California catchment. Earth Surface Processes and Landforms 30, 813–821.
Cooper, S.R., Brush, G.S., 1991. Long-term history of Chesapeake Bay anoxia. Science 254, 992–996.
Coulter Corporation, 1994. Coulter LS Series, Product Manual. Coulter Corporation, Miami, FL.
de Carvalho, G.S., Granja, H.M., Loureiro, E., Henriques, R., 2006. Late Pleistocene and Holocene environmental changes in the coastal zone of northwestern Portugal. Journal of Quaternary Science 8, 859–877.
Defries, R.S., 1986. Effects of Land-use History on Sedimentation in the Potomac Estuary, Maryland. U.S. Geological Survey Water Supply Paper 2234-K.
Duck, R.W., 1994. Applications of the QDa-Md method of environmental discrimination to particle size analyses of fine sediments by pipette and sedigraph methods: a comparative study. Earth Surface Processes and Landforms 19, 525–529.
Ember, L.M., Williams, D.F., Morris, J.T., 1987. Processes that influence carbon isotope variations in salt marsh sediments. Marine Ecology Progress Series 36, 33–42.
Erlich, R., 1983. Size analysis wears no clothes, or have moments come and gone! Journal of Sedimentary Petrology 53, 1.
Faegri, R.I., Iversen, J., 1975. Textbook of Pollen Analysis, third ed. Hafner Press, New York, NY, p. 295.
Farnsworth, K.L., Milliman, J.D., 2003. Effects of climatic and anthropogenic change on small mountainous rivers: the Salinas River example. Global and Planetary Change 39, 53–64.
Fieller, N.R.J., Gilbertson, D.D., Olbricht, W., 1984. A new method for environmental analysis of particle size distribution data from shoreline sediments. Nature 311, 648–651.
Fieller, N.R.J., Flenley, E.C., Olbricht, W., 1992. Statistics of particle size data. Applied Statistics 41, 127–146.
Finney, B.P., Huh, C.A., 1989. History of metal pollution in the southern California Bight: an update. Environmental Science and Technology 23, 294–303.
Folk, R.L., 1974. Petrology of Sedimentary Rocks. Hemphill, Austin, TX, p. 184.
Folk, R.L., Ward, W.C., 1957. Brazos River bar: a study in the significance of grain size parameters. Journal of Sedimentary Petrology 27, 3–26.
Friedman, G.M., 1967. Dynamic processes and statistical parameters compared for size frequency distribution of beach and river sands. Journal of Sedimentary Petrology 37, 327–354.
Friedman, G.M., Sanders, J.E., 1978. Principles of Sedimentology. Wiley, New York.
Gale, S.J., Hoare, P.G., 1991. Quaternary sediments: petrographic methods for the study of unlithified rocks. Wiley, New York, NY, p. 323.
Glaister, R.P., Nelson, H.W., 1974. Grain-size distributions, an aid in facies identification. Bulletin of Canadian Petrology and Geology 22, 203–240.
Goñi, M.A., Monacci, N., Gisewhite, R., Crockett, C., Nittrouer, C., Ogston, A., Alin, S.R., Aalto, R., 2008. Terrigenous organic matter in sediments from the Fly River delta-clinoform system (Papua New Guinea). Journal of Geophysical Research 113, F01S10.
Gonneea, M.E., Paytan, A., Herrera Silveira, J.A., 2004. Tracing organic matter sources and carbon burial in mangrove sediments over the past 160 years. Estuarine Coastal and Shelf Science 61, 211–227.
Gray, A.B., Pasternack, G.B., Watson, E.B., 2010. Hydrogen peroxide treatment effects on the particle size distribution of alluvial and marsh sediments. The Holocene 20, 293–301.
Greenwood, B., 1969. Sediment parameters and environment discrimination: an application of multivariate statistics. Canadian Journal of Earth Sciences 6, 1347–1358.
Hartmann, D., Christiansen, C., 1992. The hyperbolic shape triangle as a tool for discriminating populations of sediment samples of closely connected origin. Sedimentology 39, 697–708.
Hermann, A.T., 1879. Field Notes of the Reservation and Examination Made in the City Lands of Monterey: Mouth of the Salinas River. Compiled by A.T. Hermman, Deputy County Surveyor, County of Santa Clara, San Jose, CA.
Heiri, O., Lotter, A.F., Lemcke, G., 2001. Loss on ignition as a method for estimating organic and carbonate content in sediments: reproducibility and comparability of results. Journal of Paleolimnology 25, 101–110.
Johnson, W.M., Rodgers, A.F., 1854. T-473–8: Topographic Descriptive Report of Pajaro and Salinas Rivers. Coast and Geodetic Survey, Department of Commerce, U.S.
Johnsson, M.J., Meade, R.H., 1990. Chemical weathering of fluvial sediments during alluvial storage: the Macuapanim Island point bar, Soilimoes River, Brazil. Journal of Sedimentary Petrology 60, 827–842.
Kapp, R.O., Davis, O.K., King, J.E., 2000. Pollen and Spores, second ed. The American Association of Stratigraphic Palynologists Foundation, College Station, TX, p. 279.
Lario, J., Spencer, C., Plater, A.J., Zazo, C., Goy, J.L., Dabrio, C.J., 2002. Particle size characterisation of Holocene back-barrier sequences from North Atlantic coasts (SW Spain and SE England). Geomorphology 42, 25–42.
MacGinitie, G.E., 1935. Ecological aspects of a California marine estuary. American Midland Naturalist 16, 629–765.
McAndrews, J.H., Berti, A.A., Norris, G., 1973. Key to Pollen and Spores of the Great Lakes Region. Royal Ontario Museum Life Sciences Miscellaneous Publications, Toronto, Canada, p. 61.
McManus, J., 1988. Grain size determination and interpretation. In: Tucker, M. (Ed.), Techniques in Sedimentology. Blackwell, UK, pp. 63–85.
Monterey County, 1909. Map Showing Moss Landing and Its Vicinity Contiguous to Monterey Bay Compiled for the Purpose of Showing Its Position Relative to the Natural Outlets and Drainage of the Salinas and Pajaro Valleys. Compiled by Lou. G. Hare, County Surveyor, Salinas, CA, 1"=1.2 miles.
Monterey County Information Technology, 2001. Aerial Photograph 1–163 (1), 36,000.
Pasternack, G.B., Brush, G.S., Hilgartner, W.B., 2001. Impact of historic land-use change on sediment delivery to a Chesapeake Bay subestuarine delta. Earth Surface Processes and Landforms 26, 409–427.
Pasternack, G.B., Watson, E.B., Wheatcroft, R., Gray, A.B., Goñi, M., 2009. Rates and Patterns of Sediment Deposition in the Salinas River Basin, Central California. Coastal and Estuarine Research Federation biennial meeting, Portland, OR, p. 19.
Poizot, E., Mear, Y., Biscara, L., 2008. Sediment trend analysis through the variation of granulometric parameters: a review of theories and applications. Earth Science Reviews 86, 15–41.
Poppe, L.J., Eliason, A.H., Fredericks, J.J., Rendigs, R.R., Blackwood, D., Polloni, C.F., 2000. Chapter 1. Grain-size analysis of marine sediments – methodology and data processing. In: Poppe, L.J., Hastings, M.E., Eliason, A.H., Fredericks, J.J., Rendigs, R.R., Blackwood, D.S. (Eds.), U.S.G.S. East-coast Sediment Analysis: Procedures, Database, and Georeferenced Displays. U.S. Geological Survey, Woods Hole, MA. U.S. Geological Survey Open File Report 00–358.
Priju, C.P., Narayana, A.C., 2007. Particle size characterization and late Holocene depositional processes in Vembanad Lagoon, Kerala: inferences from suite statistics. Journal of the Geological Society of India 69, 311–318.
Reavie, E.D., Baratono, N.G., 2006. Multi-core investigation of a lotic bay of Lake of the Woods (Minnesota, USA) impacted by cultural development. Journal of Paleolimnology 38, 137–156.
Sahu, B.K., 1964. Depositional mechanisms from the size analysis of clastic sediments. Journal of Sedimentary Petrology 34, 73–83.
Sedimentation Seminar, 1981. Comparison of methods of size analysis for sands of the Amazon-Solimijes Rivers, Brazil and Peru. Sedimentology 28, 123–128.
Smith, R.I., 1953. The distribution of the polychaete *Neanthes lighti* in the Salinas River Estuary, California, in relation to salinity, 1948-1952. Biological Bulletin 105, 335–347.
Stockmarr, J., 1971. Tablets with spores used in absolute pollen analysis. Pollen et Spores 13, 615–621.
Sutherland, R.A., Lee, C., 1994. Discrimination between coastal subenvironments using textural characteristics. Sedimentology 41, 1133–1145.
Switzer, A.D., Pucillo, K., Haredy, R.A., Jones, B.G., Bryant, E.A., 2005. Sea-level, storms or tsunami: enigmatic sand sheet deposits in a sheltered coastal embayment from southeastern Australia. Journal of Coastal Research 21, 655–663.
Tanner, W.F., 1991a. Suite statistics: the hydrodynamic evolution of the sediment pool. In: Syvitski, J.P.M. (Ed.), Principles, Methods and Applications of Particle Size Analysis. Cambridge University Press, Cambridge, UK, pp. 225–236.
Tanner, W.F., 1991b. Application of suite statistics to stratigraphy and sea-level changes. In: Syvitski, J.P.M. (Ed.), Principles, Methods and Applications of Particle Size Analysis. Cambridge University Press, Cambridge, UK, pp. 283–292.
Trask, J.B., 1854. California State Geologist's Report on the Geology of the Coast Mountains and Part of the Sierra Nevada: Embracing Their Agricultural Resources and Mineral Productions. California Geological Survey, Sacramento, CA, p. 91.
United States Coast Survey, June 1854. Map of a part of the coast of California from the Salinas River southward. No. 478. Surveyed 1, 10,000.
United States Coast and Geodetic Survey, 1889. Pacific coast from Point Pinos to Bodega Head 1, p. 200,000. California.
United States Coast and Geodetic Survey, 1910. Monterey Bay, Salinas River Southward, p. 10,000. No. 478a 1.
United States Coast and Geodetic Survey, 1926. Map of Monterey Bay.
U.S. Department of Agriculture, 1949. Aerial Photograph ABG-17F-204 1, 21,000.
U.S. Department of Commerce, 1966. United States – West coast, California, Monterey Bay. Mercator Projection 1, 50,000.
U.S. Geological Survey, 2010. USGS 11152500 Salinas R Nr Spreckles, CA. National water information system web interface. online dataset. http://waterdata.usgs.gov/nwis/nwisman/?site_no=11152500.
Vincent, P., 1986. Differentiation of modern beach and coastal dune sands-a logistic regression approach using the parameters of the hyperbolic function. Sedimentary Geology 49, 167–176.
WAC Corporation, 1985. Aerial Photograph 14-113 (1), 31,680.
Wang, H.J., Bi, N.S., Saito, Y., Wang, Y., Sun, X.X., Zhang, J., Yang, Z.S., 2010. Recent changes in sediment delivery by the Huanghe (Yellow River) to the sea: causes and environmental implications in its estuary. Journal of Hydrology 391, 302–313.
Watson, F., Newman, W., Anderson, T., Alexander, S., Kozlowski, D., 2001. Winter Water Quality of the Carmel and Salinas Lagoons, Monterey, California: 2000/2001. Report to Monterey County Water Resources Agency, California. Report No. WI-2001-01. The Watershed Institute, Seaside, CA, p. 42. http://ccows.csumb.edu/pubs/reports/CCoWS_LagoonBreaching2001_010403.pdf.
Weltje, G.J., von Eynatten, H., 2004. Quantitative provenance analysis of sediments: review and outlook. Sedimentary Geology 171, 1–11.
Wheatcroft, R.A., Butman, C.A., 1997. Spatial and temporal variability in aggregated grain-size distributions, with implications for sediment dynamics. Continental Shelf Research 17, 367–390.
Zhou, J., Wu, Y., Zhang, J., Kang, Q., Liu, Z., 2006. Carbon and nitrogen composition and stable isotope as potential indicators of source and fate of organic matter in the salt marsh of the Changjiang Estuary, China. Chemosphere 65, 310–317.